remote sensing

MDPI

Article

Detection of Individual Corn Crop and Canopy Delineation from Unmanned Aerial Vehicle Imagery

Freda Dorbu [1] and Leila Hashemi-Beni [2,*]

[1] Department of Computational Data Science and Engineering, North Carolina A&T State University, Greensboro, NC 27411, USA; fedorbu@aggies.ncat.edu
[2] Geomatics Program, College of Science and Technology, North Carolina A&T State University, Greensboro, NC 27411, USA
* Correspondence: lhashemibeni@ncat.edu

Abstract: Precise monitoring of individual crop growth and health status is crucial for precision agriculture practices. However, traditional inspection methods are time-consuming, labor-intensive, prone to human error, and may not provide the comprehensive coverage required for the detailed analysis of crop variability across an entire field. This research addresses the need for efficient and high-resolution crop monitoring by leveraging Unmanned Aerial Vehicle (UAV) imagery and advanced computational techniques. The primary goal was to develop a methodology for the precise identification, extraction, and monitoring of individual corn crops throughout their growth cycle. This involved integrating UAV-derived data with image processing, computational geometry, and machine learning techniques. Bi-weekly UAV imagery was captured at altitudes of 40 m and 70 m from 30 April to 11 August, covering the entire growth cycle of the corn crop from planting to harvest. A time-series Canopy Height Model (CHM) was generated by analyzing the differences between the Digital Terrain Model (DTM) and the Digital Surface Model (DSM) derived from the UAV data. To ensure the accuracy of the elevation data, the DSM was validated against Ground Control Points (GCPs), adhering to standard practices in remote sensing data verification. Local spatial analysis and image processing techniques were employed to determine the local maximum height of each crop. Subsequently, a Voronoi data model was developed to delineate individual crop canopies, successfully identifying 13,000 out of 13,050 corn crops in the study area. To enhance accuracy in canopy size delineation, vegetation indices were incorporated into the Voronoi model segmentation, refining the initial canopy area estimates by eliminating interference from soil and shadows. The proposed methodology enables the precise estimation and monitoring of crop canopy size, height, biomass reduction, lodging, and stunted growth over time by incorporating advanced image processing techniques and integrating metrics for quantitative assessment of fields. Additionally, machine learning models were employed to determine relationships between the canopy sizes, crop height, and normalized difference vegetation index, with Polynomial Regression recording an R-squared of 11% compared to other models. This work contributes to the scientific community by demonstrating the potential of integrating UAV technology, computational geometry, and machine learning for accurate and efficient crop monitoring at the individual plant level.

Keywords: precision agriculture; computational geometry; canopy height model; Voronoi; local maximum; segmentation

Citation: Dorbu, F.; Hashemi-Beni, L. Detection of Individual Corn Crop and Canopy Delineation from Unmanned Aerial Vehicle Imagery. *Remote Sens.* **2024**, *16*, 2679. https://doi.org/10.3390/rs16142679

Academic Editors: Leonardo Conti, Diego Bedin Marin, Giuseppe Rossi and Gabriel Araújo e Silva Ferraz

Received: 15 June 2024
Revised: 6 July 2024
Accepted: 17 July 2024
Published: 22 July 2024

1. Introduction

The integration of precision agriculture (PA) stands to significantly enhance agricultural efficiency, especially considering the expected global population rise and increasing demands for food security. Focusing on economically crucial crops like corn, PA employs advanced tools such as remote sensing (RS), Geographic Information Systems (GISs), and Global Positioning System (GPS) to optimize field management. This approach aims to

maximize resource efficiency and minimize waste, thereby increasing crop yields and promoting environmental sustainability. Despite its potential, the adoption of PA is hindered by financial constraints and technical complexities, which deter stakeholder engagement [1–3].

Remote sensing has emerged as a dependable method for monitoring fields, utilizing UAVs, piloted aircraft, and satellites for data collection [4,5]. UAVs are becoming increasingly vital in agriculture, thanks to their ability to carry diverse sensors and provide high-resolution, cost-effective images [6]. Even with their limited flight time, for localized, short-term missions requiring rapid deployment, UAVs offer more flexibility than satellites and piloted aircraft [7]. UAVs play a critical role in crop monitoring, offering detailed insights into individual crop characteristics, biomass, and overall field uniformity [8–10].

However, there is a significant gap in applying existing remote sensing technologies for precisely monitoring and managing individual crop characteristics, especially in understanding and optimizing the complex canopy structures of crops like corn. This gap underscores the need for more sophisticated, efficient, and widely applicable methodologies in crop management. This study proposes a novel methodology that harnesses the power of UAV imagery and computational geometry for individual corn plant monitoring. The approach utilizes the Canopy Height Model (CHM) [5,11–15] derived from the difference between the Digital Terrain Model (DTM), the Digital Surface Model (DSM) [5,16–21], and the modified Voronoi diagram. Some research work [22–24] enable efficient corn canopy detection and delineation. This modified Voronoi diagram incorporates domain-specific knowledge about corn plant spacing and spectral data such as Excess Green (ExG) and normalized difference vegetation index (NDVI) to filter out noise elements like soil, background, and shadows, leading to enhanced accuracy and efficiency in agricultural monitoring and management [25–27].

2. Materials and Methods

This research employed a workflow leveraging Python 3.12.3 scripting for automation, Agisoft Photoscan 2.1.2 for detailed 3D reconstruction (photogrammetry), and ArcGIS Pro 3.0 for comprehensive spatial analysis and compelling visualization of the generated crop models. This integrated approach streamlined the complex data processing and analysis workflows, ultimately facilitating precise crop modeling (Figure 1).

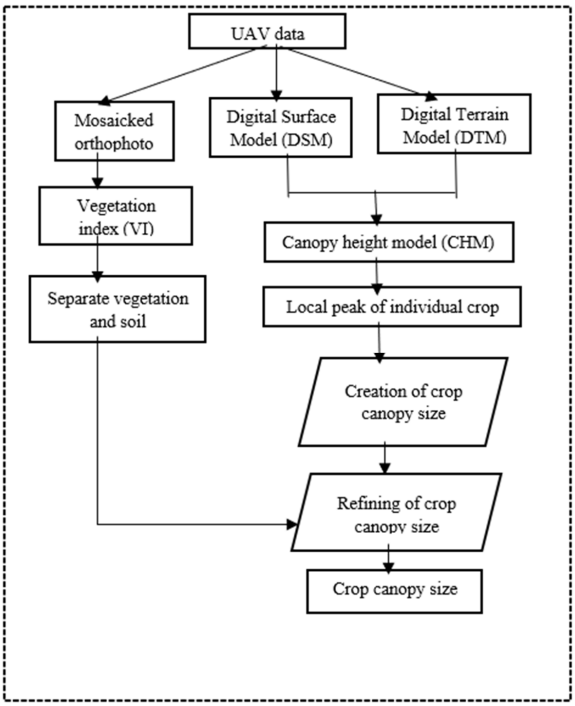

Figure 1. Automated framework for crop mapping and canopy characterization.

2.1. UAV Data Collection

This research employed a comprehensive approach to data acquisition, leveraging high-resolution RGB time-series imagery throughout the entire crop cultivation phase. The data collection spanned from the initial planting on 30 April to the final harvest on 11 August, ensuring a complete temporal record of the crop's growth and development specific to our region of study. The primary imaging platform utilized in this study was a DJI Phantom 4 Pro Unmanned Aerial Vehicle (UAV) equipped with a 4K UHD 2160p RGB camera (DJI, Shenzhen, China). This state-of-the-art UAV system was chosen for its ability to capture exceptionally high-resolution RGB imagery, which is crucial for accurate crop modeling and analysis. To further explore the potential benefits of additional spectral information, this research also acquired imagery using a separate UAV equipped with a near-infrared (NIR) sensor. NIR imagery has proven valuable in various agricultural applications, as it can provide insights into crop health, stress levels, and biomass estimation [28]. To determine the optimal flight altitude for accurate crop modeling, the research conducted flights at two different elevations: 40 m and 70 m above ground level. This approach allowed for a comprehensive evaluation of the trade-offs between spatial resolution and field coverage, ensuring that the final methodology would strike the right balance between these factors. By employing a multi-sensor approach and capturing data at various altitudes, this research aimed to develop a robust and adaptable methodology for individual corn plant monitoring. The high-resolution RGB imagery provided detailed spatial information for plant identification and segmentation, while the NIR data offered complementary spectral information for understanding plant health and physiological characteristics. Images acquired from the NIR sensor were resampled for further analysis with RGB sensor images. Moreover, the time-series nature of the data collection allowed us to track the growth and development of individual plants throughout the entire crop cycle. This longitudinal approach enabled the research team to investigate the dynamic changes in plant characteristics over time, providing valuable insights into the impact of environmental factors, management practices, and phenological stages on crop growth and yield.

2.2. Canopy Height Model (CHM) Generation and Individual Plant Identification

The imagery captured at varying flight altitudes underwent Structure from Motion (SFM) processing, which is a powerful technique for constructing orthophotos and three-dimensional crop models from overlapping two-dimensional images. SFM incorporates feature matching and camera alignment algorithms [29] to generate accurate Digital Surface Models (DSMs) and Digital Terrain Models (DTMs). Generating an accurate Digital Surface Model (DSM) and Digital Terrain Model (DTM) was pivotal in this endeavor. The DSM, depicting crop elevation, and the DTM, representing bare ground elevation, were derived from Unmanned Aerial Vehicle (UAV) images acquired before planting, when the field was bare, and from subsequent time-series imagery. The accuracy of crop height estimation and crop detection heavily relied on the quality of the DSM, which accurately represents the crop surface and ensures precise characterization of the study field. The accuracy of our generated DSM was calculated by comparing it with Ground Control Points (GCPs) from our field of study, which indicated that the DSM was representative of the field.

While this research utilized time-series data, imagery captured at a single flight altitude on 11 August, coinciding with mature crops, was employed for this specific analysis. This decision was made to isolate the impact of canopy structure on a specific growth stage, in this case, the mature stage of the crop cycle. By focusing on a single time point, the analysis could effectively investigate the influence of the intricate canopy structure on individual crop identification and monitor without the confounding effects of temporal variations in growth stages.

In our study, we developed a Canopy Height Model (CHM) to aid in the identification of individual crops by calculating the difference between the DSM, which captures the crop elevation, and the DTM, which represents the elevation of the bare earth. This calculation

effectively highlights the height of the crops, discounting the elevation of the terrain [23,30]. This calculation is represented by the following equation:

$$\text{Canopy height model} = \text{DSM} - \text{DTM} \quad (1)$$

To further enhance the CHM's accuracy, a user-defined threshold based on the typical mature corn height, often exceeding 3 m, was applied. This filtering step removed irrelevant noise such as soil and shadows and retained essential features related to vegetation. By leveraging the known characteristic height of mature corn, the methodology effectively isolated the relevant height information, increasing the reliability of the subsequent analyses. This preprocessing step, encompassing height-based filtering, not only improved analytical accuracy but also optimized computational efficiency. By reducing the amount of irrelevant data and noise, the preprocessing stage streamlined the subsequent analyses, minimizing the computational resources required and enabling more efficient processing pipelines. Overlaying the refined CHM onto orthophotos allowed for a visual evaluation of crop heights via their spectral characteristics, facilitating a detailed and effective analysis of the crop data. This integration of height information with high-resolution orthoimagery provided a comprehensive representation of the field, enabling researchers to visually inspect and validate the crop height estimates in the context of the spectral signatures and spatial patterns observed in the imagery.

A unique methodology was utilized for the detection of individual crops within this study by pinpointing each crop's local peak height through the CHM. This was accomplished by deploying a local maxima function on the CHM, designating a pixel as a local maximum when its value is greater than or equal to the values of its surrounding pixels, marking the apex of crops. This approach leveraged the fact that individual crop plants would exhibit localized height maxima within the CHM, representing the highest point of their canopy structure. Various sizes of moving windows were tested on the CHM to determine the most suitable window size for this analysis, with a 10×10 window size proving most effective in accurately identifying local peak heights and discerning corn crops. The choice of window size is crucial, as it determines the spatial extent over which the local maxima are evaluated, affecting the ability to distinguish individual crop elements accurately. The validity of this approach was confirmed through a comparison of the produced local maxima map with the original CHM, ensuring accurate crop identification. This validation step provided confidence in the methodology's ability to reliably detect and locate individual crops within the study area. The local maximum map was then transformed into point data to detail the specific heights of individual crops, enabling further quantitative analyses and modeling of crop characteristics. The equation representing the local maxima function is as follows:

$$MaxValue(c_{i,j}) = max_{x=i-5}^{i+4} max_{y=j-5}^{j+4} R_{x,y} \quad (2)$$

where the $MaxValue(c_{i,j})$ is the maximum value assigned to the cell at position (i,y) in the output raster map. $R_{x,y}$ represents the value of the cell in the input CHM and the ranges $x = i - 5$ to $x = i + 4$ and $y = j - 5$ to $y = j + 4$ define the 10×10 window around cell $C_{i,j}$, considering a zero-based index. If the CHM is 1-based, the indices would adjust accordingly.

To validate the effectiveness of the developed methodology for individual crop detection, the number of 13,000 crops identified using the local maxima approach was compared to manual crop estimations of 13,050 performed by human observers in the field. This comparison served as a crucial step in assessing the accuracy and reliability of the automated crop detection process. Manual crop estimation is a labor-intensive and time-consuming process that involves human observers physically counting and recording the number of individual crop plants within designated areas of the field. This process is typically considered the ground truth reference, as it relies on direct visual observation and human judgment, albeit subject to potential errors and biases. By comparing the number of crops

identified by the automated methodology to the manual estimates, we aimed to evaluate the performance of the developed approach in terms of its ability to accurately detect and count individual crop plants. This comparison provided insights into the potential under- or overestimation of crop numbers by the automated method, as well as its consistency across different field conditions and crop growth stages.

The validation process used in this study involved calculating the Mean Absolute Error (MAE) and Root Mean Squared Error (RMSE) to measure the average magnitude of errors between the aerial counts and the manual counts, as well as the accuracy percentage to quantify the discrepancies between the automated and manual crop counts. Additionally, visualizations, such as scatter plots and bar plots, were employed to assess the correlation and agreement between the two methods of crop identification. Our automated crop detection methodology consistently produced crop counts that were in close agreement with the manual estimates, providing confidence in the reliability and robustness of the developed approach. This validation step is crucial in the context of precision agriculture practices, as accurate crop counts and spatial distributions are essential for informed decision-making processes, such as yield estimation, resource allocation, and targeted interventions. By comparing the automated methodology with ground truth data, researchers can assess the suitability and applicability of the developed approach in real-world agricultural settings, ultimately contributing to the advancement of sustainable and efficient crop management practices.

2.3. Canopy Size Delineation and Refinement

Building upon the previously generated Canopy Height Model (CHM) and individual crop identification, our methodology for delineating canopy sizes leverages a synergistic integration of remote sensing data, computational geometry algorithms, and a vegetation index (e.g., NDVI) to achieve accurate delineation and quantification of individual crop canopies. This approach centers around a local peak height map derived from the CHM, effectively pinpointing the apical regions of each crop within the study area. Leveraging the principles of computational geometry, we employ a Voronoi tessellation algorithm [31,32] on the local peak height map. This technique partitions the field into a set of polygonal regions, where each region encloses the area closest to a specific local maximum point, effectively representing the apex of an individual crop plant. This approach is particularly advantageous for delineating individual canopies as it respects the spatial distribution of the crops, ensuring that each canopy is represented by a distinct polygon that accurately captures its boundaries. This spatially aware segmentation enables precise and detailed analysis of individual crop plants, facilitating the monitoring of their growth, health, and development over time. Mathematically, the Voronoi diagram (Figure 2) can be defined as follows:

$$\mathcal{V}(p) = \left\{ q \in \mathbb{R}^d : |q - p| < |q - p'|, \forall p' \in P - p \right\} \quad (3)$$

where V(p) denotes the Voronoi region associated with the local maximum point p, and P represents the set of all local maximum points within the field. The equation essentially defines the Voronoi region V(p) as the set of points q in d-dimensional Euclidean space that are closer to p than to any other local maximum point p' in P, excluding p itself. The Euclidean distance metric, given by the following equation:

$$\left(\sum_{i=1}^{d} (p_i - q_i)^2 \right)^{1/2} \quad (4)$$

serves as the basis for determining the proximity of points within the Voronoi tessellation, ensuring an accurate and unbiased partitioning of the field into individual crop canopy regions.

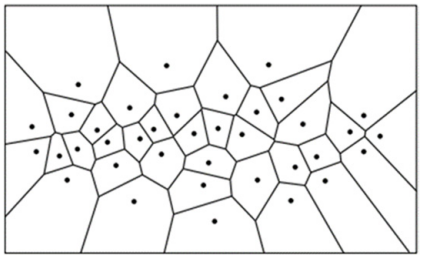

Figure 2. A Voronoi diagram delineating points acquired from [31].

While effective for delineating individual canopies, Voronoi diagrams may include both vegetation and soil, particularly at different growth stages. This can lead to overestimation of canopy size. To address this and ensure more precise estimates, we developed a refinement method that utilizes vegetation indices (VIs). These VIs leverage specific spectral characteristics of vegetation in multispectral imagery to effectively separate vegetation from non-vegetative elements. The orthophotos generated during the preprocessing phase play a crucial role in creating VIs. We evaluated various VIs, including the normalized difference vegetation index (NDVI) (Equation (5)), Green Chromatic Coordinate (GCC) (Equation (6)), and Excess Green (ExG) (Equation (7)), to determine the most suitable option for refining canopy size estimates in our study [33].

$$\mathrm{NDVI} = \frac{(\mathrm{NIR} - \mathrm{Red})}{(\mathrm{NIR} + \mathrm{Red})} \tag{5}$$

where NIR is the near-infrared reflectance band with higher reflectance in healthy vegetation compared to soil, and red band reflectance has lower reflectance in vegetation compared to soil [34].

$$\mathrm{GCC} = \mathrm{G}/(\mathrm{R} + \mathrm{G} + \mathrm{B}) \tag{6}$$

$$\mathrm{ExG} = (2 \times \mathrm{G}) - \mathrm{R} - \mathrm{B} \tag{7}$$

where G, R, and B represent the green, red, and blue bands of the orthophoto, respectively. The ExG index was selected for the refinement process because of its effectiveness in vegetation segmentation [35] and its ability to distinguish vegetation from soil and other features within our specific project context. The excess green index exploits the unique spectral characteristics of vegetation, specifically the higher reflectance in the green region compared to the red and blue regions, enabling a precise separation of vegetation from soil and other non-vegetative elements. Figure 3 is an example of the indices created by us for the refinement of the canopy sizes.

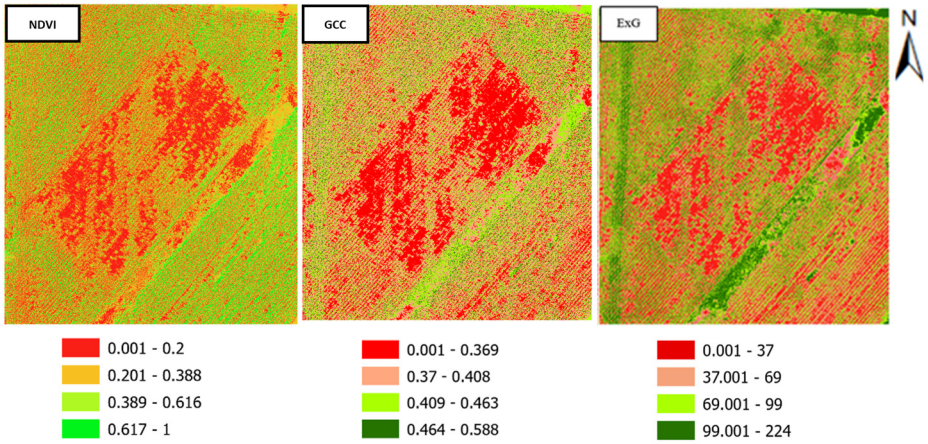

Figure 3. A map of the estimated NDVI, GCC and ExG indices.

The validation of the proposed refinement method for individual crop canopy size estimation was conducted through a multi-faceted approach, leveraging expert knowledge, visual inspection, and statistical analysis. The primary objective was to assess the accuracy and effectiveness of the refinement process in accurately delineating crop canopies and separating vegetation from non-vegetative components. The locations of individually detected crops, identified through the Canopy Height Model (CHM) and local maxima detection, were compared with the pre-existing planting schema. The planting schema provides knowledge about the specific crop species, including the expected mature canopy size range, planting arrangement (e.g., row spacing), and spatial distribution patterns. This comparison leveraged expert knowledge to validate the accuracy of crop identification and location, ensuring that the detected crops align with the expected planting layout.

The top crop point, representing the apex of each identified crop, and the refined canopy size delineation were overlaid on the original high-resolution RGB imagery. This visual overlay enabled a qualitative assessment of the delineated canopy boundaries, ensuring they accurately corresponded to the visible crop canopies in the imagery. Additionally, a non-parametric statistical test, the Mann–Whitney U test, was conducted to assess the statistical significance of the difference in canopy sizes before and after the refinement process. The Mann–Whitney U test is a robust non-parametric alternative to the *t*-test, appropriate for comparing two independent samples without making assumptions about the underlying distribution of the data. The test was conducted with a significance level of 0.05, which is a commonly accepted threshold for statistical significance in scientific research. The null hypothesis of the test was that there is no significant difference between the means of the original canopy sizes (before refinement) and the refined canopy sizes (after the vegetation index-based refinement process). The *p*-value obtained from the test indicates the probability of observing such a difference in means if the null hypothesis is true. A *p*-value less than 0.05 suggests that there is a statistically significant difference between the means, indicating that the refinement process had a significant impact on the accuracy of the estimated canopy sizes. This multi-pronged validation approach ensured a comprehensive assessment of the refinement method's effectiveness.

2.4. Machine Learning Integration

To explore the influence of NDVI and crop height on canopy size, and subsequently analyze their impact on crop yield by leveraging NDVI's established correlation with yield, we employed several machine learning models, utilizing canopy size as the dependent variable and crop height and NDVI as independent variables; the models included Polynomial Regression (Degree 2), which fits a quadratic polynomial equation to capture non-linear relationships; Support Vector Machine (SVM) with a Radial Basis Function (RBF) kernel that maps input data into a higher-dimensional feature space to identify non-linear relationships; Gradient Boosting Machine, which is an ensemble technique that combines multiple weak learners (decision trees) in an iterative process to correct errors of previous learners; Ridge Regression, which introduces L2 regularization to mitigate multicollinearity and prevent overfitting; Linear Regression aiming to find the best-fitting straight-line relationship; Lasso Regression, which employs L1 regularization for feature selection and sparse modeling; K-Nearest Neighbors (KNN), which predicts canopy size based on the weighted average of the k closest training data points using a distance metric; Random Forest, which constructs multiple decision trees on random subsets of data and features with the final prediction being the average; and decision tree, which recursively partitions the input space based on independent variables to predict the dependent variable. An Ordinary Least Squares (OLS) analysis further investigated the relationship between canopy size and its predictors, with the OLS estimator equation being the following:

$$\hat{B} = \left(x^T x\right)^{-1} x_y^T \tag{8}$$

where y is the dependent variable (canopy size), X is the matrix of independent variables (crop height and NDVI), β is the vector of coefficients, and ε is the error term. Leveraging NDVI, crop height, and estimated canopy sizes for the 13,000 aerially counted crops, we employed machine learning models to predict canopy sizes. The models' performance was evaluated using R-squared, indicating the proportion of variance in canopy size explained by the models, and Mean Absolute Error (MAE) to assess the average magnitude of prediction errors [36–38].

2.5. Evaluation Metrics

To evaluate the performance of the quantitative analysis conducted in this study, three key metrics were employed: Mean Absolute Error (MAE), Root Mean Squared Error (RMSE), and R-squared (R^2). These metrics provide valuable insights into the accuracy, precision, and explanatory power of the models and analyses employed, enabling a comprehensive assessment of the methodology's effectiveness.

Mean Absolute Error (MAE) is a widely used metric that measures the average magnitude of the errors in a set of predictions, without considering their direction. It is calculated as the average over the test sample of the absolute differences between the predicted and actual values, as represented by the following equation:

$$MAE = \frac{1}{n}\sum_{i=1}^{n}|y_i - \hat{y}_i| \quad (9)$$

where y_i is the actual value, $\hat{y}_i$ is the predicted value, and n is the number of observations. MAE is particularly useful because it provides a straightforward interpretation in terms of error magnitude, offering an intuitive understanding of the average deviation between predicted and observed values.

Root Mean Squared Error (RMSE) is another commonly employed metric that quantifies the average magnitude of the errors, considering the direction of the errors. RMSE is calculated as the square root of the average of the squares of the errors, as represented by the following equation:

$$RMSE = \sqrt{\frac{1}{n}\sum_{i=1}^{n}(y_i - \hat{y}_i)^2} \quad (10)$$

RMSE is sensitive to outliers and gives a higher weight to larger errors due to the squaring of the errors. This characteristic can be beneficial in certain contexts where large errors are particularly undesirable, as it effectively penalizes models or analyses that produce significant outliers.

R-squared (R^2), also known as the coefficient of determination, is a statistical measure that represents the proportion of the variance for a dependent variable that is explained by an independent variable or variables in a regression model. It provides an indication of the goodness of fit and, therefore, a measure of how well unseen samples are likely to be predicted by the model, relative to the mean of the observed data. R^2 is calculated using the following equation:

$$R^2 = 1 - \frac{\sum_{i=1}^{n}(y_i - \hat{y}_i)^2}{\sum_{i=1}^{n}(y_i - \overline{y})^2} \quad (11)$$

where y_i is the actual value, $\hat{y}_i$ is the predicted value, and $\overline{y}$ is the mean of the actual values. R^2 ranges from 0 to 1, with higher values indicating a better fit of the model to the data and a greater ability to explain the variance in the dependent variable.

In the context of this study, these metrics played a crucial role in evaluating the performance of the various machine learning models and statistical analyses employed. The MAE and RMSE values provided insights into the magnitude of errors and the overall accuracy of the predictions, enabling comparisons between different models and methodologies. Lower values of MAE and RMSE generally indicate higher accuracy and precision in the analysis. Furthermore, the R^2 values were instrumental in assessing the explanatory power of the models, particularly in the context of exploring the influence of NDVI and crop height

on canopy size and yield. Higher R^2 values suggest that the models effectively capture a larger proportion of the variance in the dependent variable (canopy size), indicating a stronger explanatory power and better predictive capabilities.

By integrating these metrics into the evaluation process, we were able to comprehensively assess the performance of our quantitative analyses, identify areas for potential improvement, and ensure the reliability and robustness of the developed methodologies. This rigorous approach to performance evaluation is essential in scientific research, as it provides a quantitative basis for validating the results, identifying limitations, and informing future refinements or alternative approaches.

3. Implementations and Results

3.1. Study Area and Data Collection

Our research site was a corn crop field situated at the North Carolina Agricultural and Technical State University's research farm in Greensboro (36.07260°N, 79.79200°W). The field measures 415 ft × 210 ft and benefits from Greensboro's favorable humid subtropical climate, with an average July temperature of 78.5°F and annual rainfall of 45 inches, ideal for corn growth (Figure 4). The Cecil soil type and an average elevation of 243 m above sea level further characterize the field. Standard agricultural practices were followed for corn planting, with winter crops strategically retained to assess their impact on subsequent corn growth. Spectral profiling of select field areas was conducted (Figure 5). This technique proved to be a valuable tool for understanding variability within the field. Spectral profiles capture the reflectance properties of different materials across various wavelengths of light. By analyzing these profiles, we can gain insights into the health, growth stage, and composition of the crops across the field. Our spectral data revealed subtle differences in nutrient uptake or water stress, allowing for targeted interventions to optimize crop health and yield.

Figure 4. Orthophoto of study area.

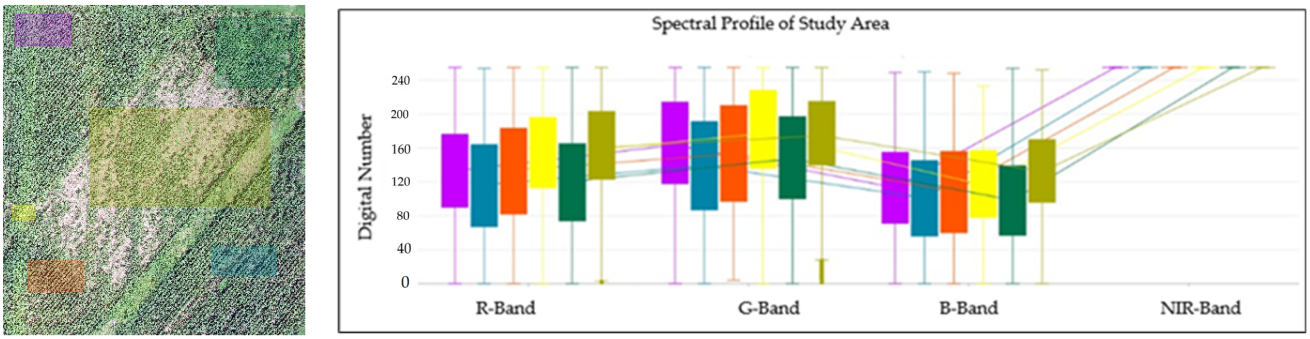

(**a**) (**b**)

Figure 5. (**a**) Randomly selected areas of the study site. (**b**) Spectral profile of randomly selected areas of the study area.

3.2. CHM Development and Crop Detection

Our investigation generated a Canopy Height Model (CHM) for the cornfield (Figure 6a). To ensure a precise representation of the mature corn canopy, the CHM underwent meticulous refinement. This refinement involved applying a height threshold specifically chosen based on the typical height range of fully grown corn at its peak growth stage. This meticulous approach effectively excluded extraneous noise from ground features or young crop variations. The resulting refined CHM provides a clear picture of the mature corn canopy distribution across the field (Figure 6b). The refined CHM served two key purposes. First, it offered a more precise representation of the mature corn canopy, ensuring that only relevant vegetation was considered in subsequent analyses. Consequently, the resulting canopy height map accurately reflects the spatial variability of the mature corn canopy, allowing us to detect patterns such as dense growth clusters, gaps in coverage, and overall canopy health across the field. Furthermore, the refined CHM facilitated a more detailed assessment of crop uniformity. This detailed assessment enabled the identification of areas with stunted growth or variations in canopy height that might indicate potential issues like pest infestation, disease outbreaks, or crop lodging. Such insights are crucial for precision agriculture, where timely intervention and targeted management practices can significantly improve yields and reduce resource waste. A 10 × 10 m focal statistical analysis was applied to the refined CHM, converting it to a point cloud representing the heights of individual corn plants. This analysis identified approximately 13,000 local peak heights, closely matching the 13,050 plants counted manually. Examining these peak height variations provided a detailed picture of crop density across the field (Figure 6c). Areas with higher concentrations of peaks indicated denser crop growth, while areas with sparse peaks suggested lower density.

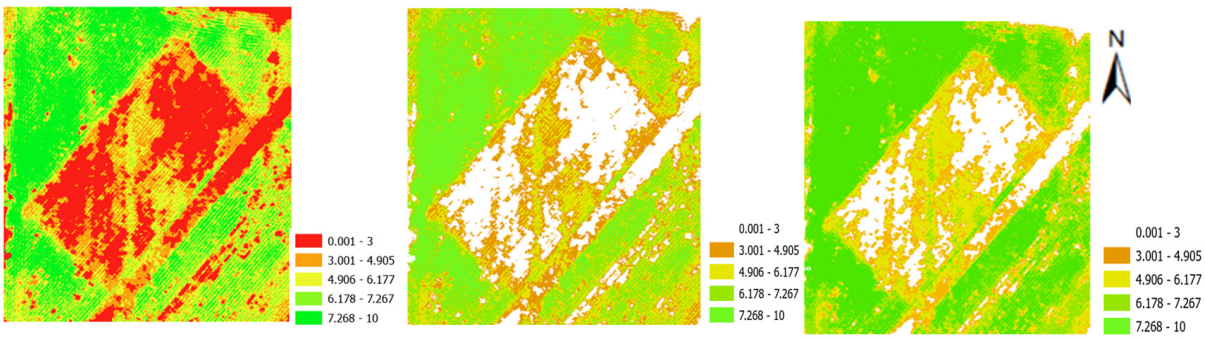

(**a**) (**b**) (**c**)

Figure 6. (**a**) Initially generated CHM. (**b**) Filtered CHM. (**c**) Local peak height. The unit of measurement for the CHM, filtered CHM, and generated local peak height maps is feet.

To evaluate the accuracy of the automated plant detection, we compared it to the manual count. This analysis revealed a Mean Absolute Error (MAE) and Root Mean Squared Error (RMSE) of 50 feet each, with an overall crop detection accuracy of 99.6%. This analytical step was visually corroborated by overlaying the resulting data points onto the orthophoto of the study area. The comparative analysis also revealed a high degree of accuracy in the representation of crop peaks within the study area, as evidenced in Figure 7.

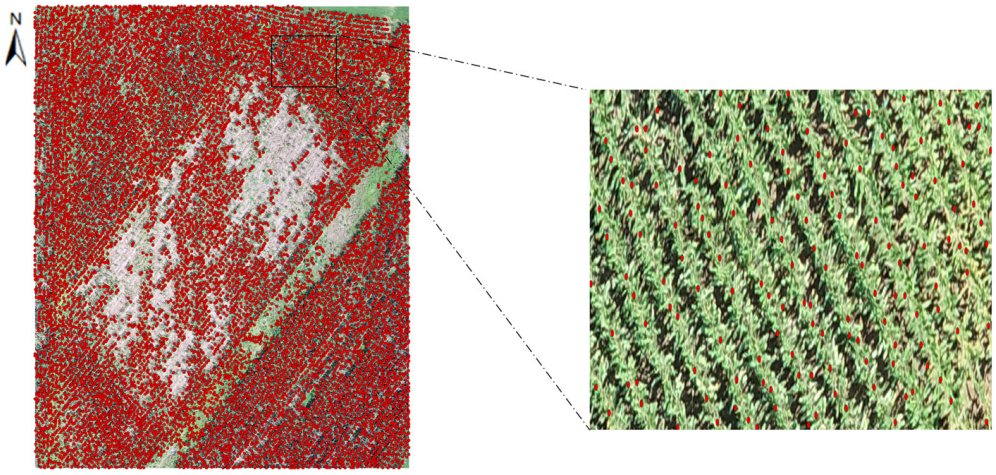

Figure 7. Local maximal results showing the peak height of each crop.

3.3. Canopy Size Estimation and Refinement

Our investigation employed an innovative approach to analyze individual corn plants and estimate canopy sizes. A Voronoi diagram, constructed based on the previously identified local peak heights from the CHM (Figure 7), facilitated the spatial partitioning of the field. This diagram essentially created a unique polygonal region surrounding each identified corn plant, providing a practical framework for further analysis. Initial estimates of canopy size using the Voronoi diagram alone revealed limitations due to the inclusion of soil and shadows within the polygonal regions (Figure 8). To address this and achieve more precise estimations, a refinement process was implemented using the Excess Green vegetation index. This index effectively distinguished between vegetative and non-vegetative elements by capitalizing on the heightened green reflectance of healthy vegetation compared to other wavelengths. By incorporating the Excess Green index created in Section 2.3, the analysis significantly improved the precision of canopy delineation. This successfully excluded soil patches, shadows, and other background elements from the calculations, resulting in a more accurate representation of individual canopy sizes (Figure 9). This combined approach, utilizing both Voronoi diagrams and the Excess Green index, allowed for a more accurate estimation of individual canopy sizes and overall crop density across the field (Figure 10). Each polygonal region was assessed, providing a clearer understanding of the spatial distribution of corn plants and the variability in canopy size.

To validate the effectiveness of the refinement process in improving canopy size estimations, a statistical analysis was conducted on the canopies generated before and after refinement. The Mann–Whitney U test, a non-parametric test suitable for comparing distributions, was employed. This test specifically compared the distributions of canopy sizes before and after the refinement process using the Excess Green vegetation index. The Mann–Whitney U test yielded a significant result, with a p-value of 0. This p-value essentially indicates that the observed difference in canopy sizes between the two groups is highly unlikely (essentially zero probability) to be due to random chance. In other words, the refinement process significantly altered the data distribution, suggesting it effectively addressed the limitations of the initial estimates. This statistically significant difference underscores the importance of the refinement process. Removing non-vegetative elements like soil and shadows significantly reduced noise in the data, leading to a more

accurate representation of the true canopy sizes. This enhanced precision is crucial for understanding the spatial variability of corn growth across the field.

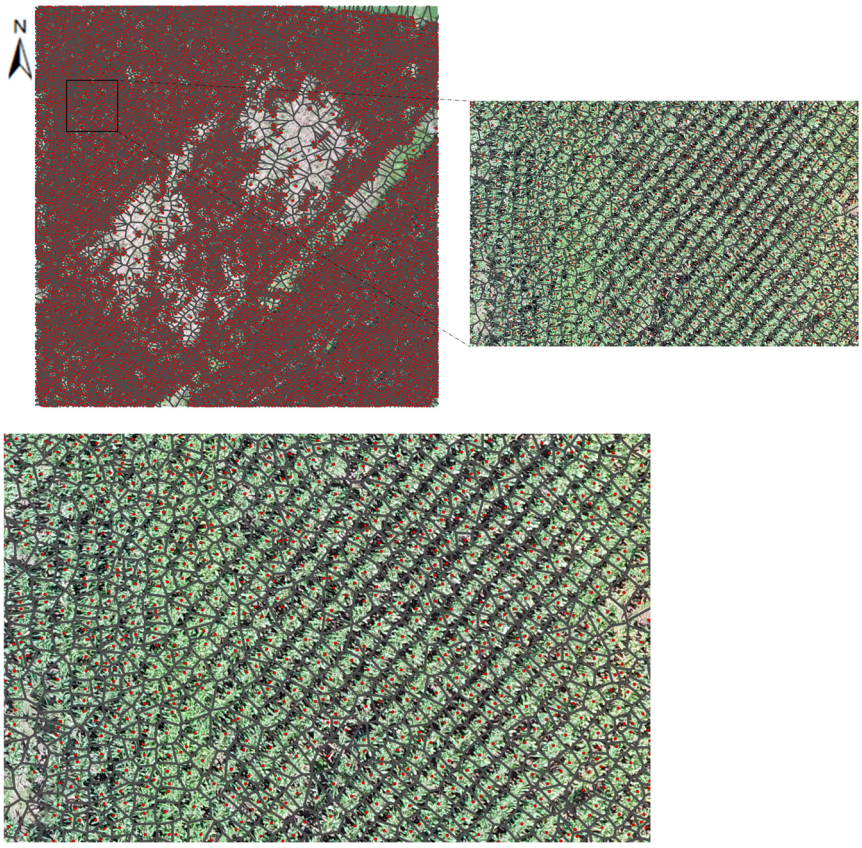

Figure 8. A Voronoi map showing the canopy sizes and the individual crop peak heights with noise.

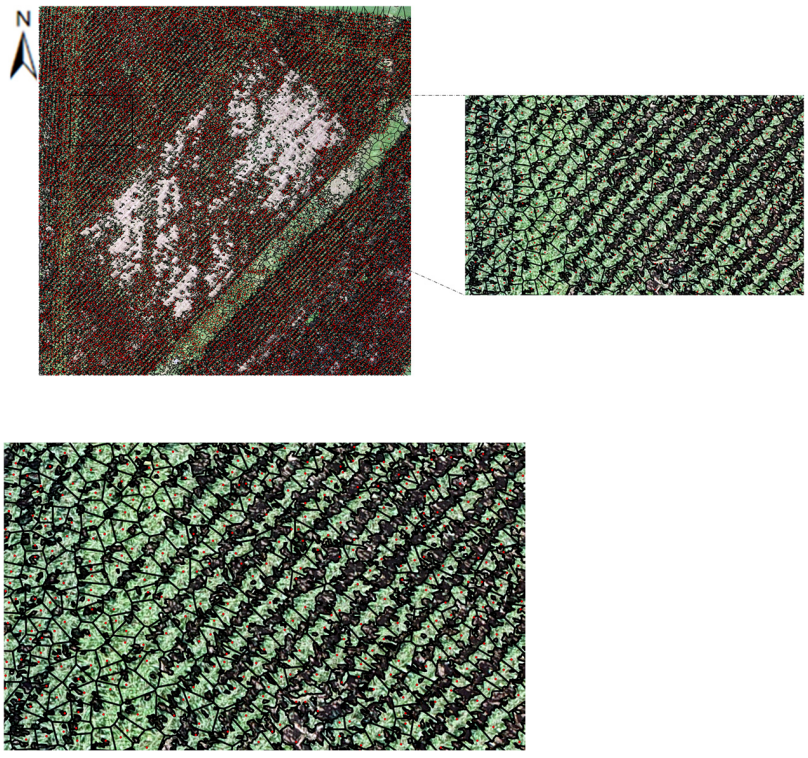

Figure 9. Refined crop canopy sizes.

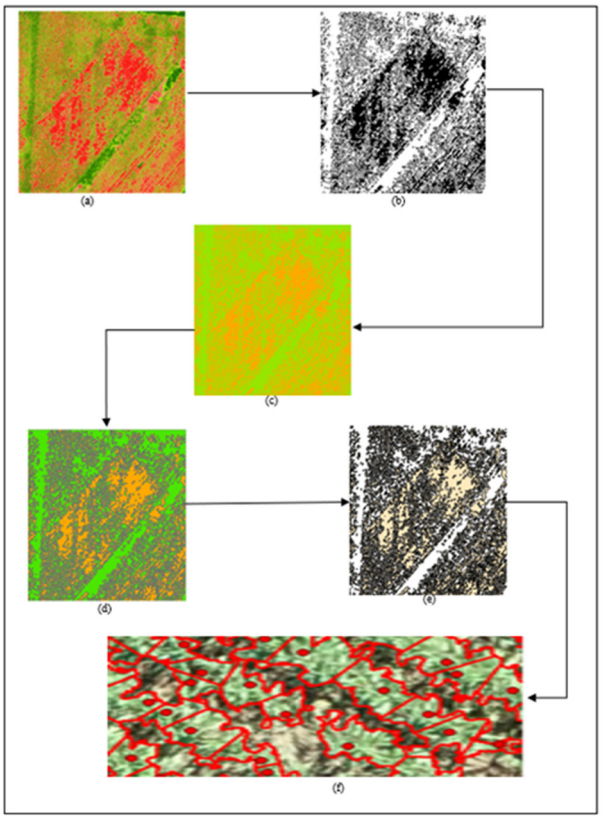

Figure 10. The refinement process of each crop canopy size from (**a**) ExG to (**b**) segmented ExG. (**c**) Reclassified segmented ExG. (**d**) Conversion of segmented ExG raster to polygon. (**e**) Soil feature selection. (**f**) Overlay of modified Voronoi on the RGB image.

Table 1 provides descriptive statistics that offer insights into the changes in canopy size delineation after refinement. The number of observations (13,000) remained constant, indicating no change in the analyzed objects. However, the mean canopy size decreased from 8.93 to 5.78 after refinement, suggesting a reduction in estimated size on average. Additionally, the standard deviation decreased from 13.86 to 12.34, indicating that the refined estimates are more tightly clustered around the mean, with less variability. Interestingly, the minimum canopy size decreased from 0.90 to 0.004, implying that the refinement process identified and retained some very small canopy sizes potentially missed initially. However, the maximum canopy size also decreased slightly, suggesting that some of the largest estimates might have been trimmed. All three quartile values (25th, 50th, and 75th percentiles) also decreased, further supporting the overall trend of a reduction in estimated canopy sizes across the distribution. In summary, the descriptive statistics suggest that the refinement process led to a general decrease in canopy size estimates, with a lower mean, reduced variability, and a shift towards smaller values. Notably, the process also retained some very small canopies potentially missed earlier. These findings indicate that the refinement process effectively addressed overestimation issues, potentially leading to more accurate and conservative estimates. However, further analysis and validation are necessary to fully assess the practical implications and accuracy of the refined canopy size estimates.

To complement the statistical analysis, a visual inspection of the canopy size distribution before and after refinement was conducted using histograms (Figure 11). These revealed a clear skew towards larger canopy sizes in the "Before" distribution, indicating a prevalence of objects with extensive canopy cover before refinement. Conversely, the "After" distribution displayed a shift towards lower canopy sizes, suggesting a potential decrease in overall size for some objects. Importantly, an overlap existed between the "Before" and "After" distributions, signifying that some objects likely maintained similar

canopy size values throughout the process. The visual analysis supports the conclusion that the refinement process may have led to a slight reduction in canopy size for a portion of the objects. Overall, this study demonstrates that the implemented refinement process significantly impacted canopy size estimations. The process likely reduced noise by removing non-vegetative elements, resulting in more accurate and conservative estimates.

Table 1. Descriptive statistics of canopy size delineation.

	Initial Canopy Size (ft)	Refined Canopy Size (ft)
Count	13,000	13,000
Mean	8.927187	5.781796
Standard deviation	13.858262	12.339383
Minimum value	0.901887	0.004016
Maximum value	348.572489	348.021710
25%	4.666112	2.715247
50%	6.177899	3.914694
75%	8.341895	5.359943

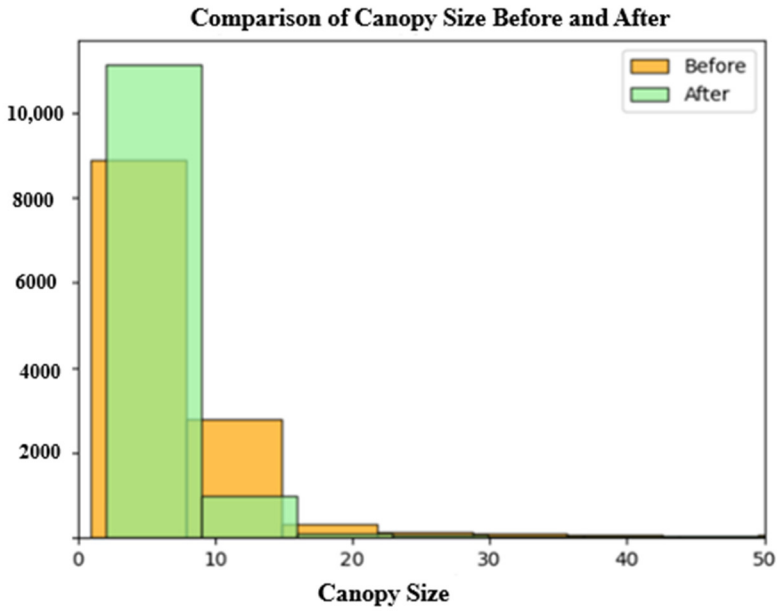

Figure 11. Influence of canopy refinement.

3.4. Statistical Analysis

This section analyzes the performance of various machine learning models trained on a dataset of 13,000 NDVI, crop height, and canopy size measurements (80% for training, 20% for testing—see Table 2) to predict canopy size. Polynomial Regression and SVM with RBF kernel exhibited the best performance, evident from their higher R-squared values and lower Mean Absolute Error (MAE). However, the relatively low R-squared values for all models suggest that NDVI and crop height alone provide limited explanatory power for canopy size variations (Figure 12). The lower MAE values for SVM and Polynomial Regression highlight their marginally better prediction accuracy. Future exploration could involve incorporating more data, feature engineering (e.g., including weather data), or alternative modeling techniques (e.g., Random Forests) to improve model performance. The Polynomial Regression model yielded an equation (Equation (8)) that captures the predicted relationship between canopy size, NDVI, and crop height. This equation incorporates linear terms for direct effects, interaction terms for combined effects, and squared terms for

non-linear effects, providing a comprehensive view of their influences on canopy size prediction.

$$y = 15.8114 - 2.2716X_1 + 0.1542X_2 + 0.1293{X_1}^2 + 0.0190X_1X_2 - 0.3584{X_2}^2 \quad (12)$$

where the y is the canopy size, the X_1 is the crop height, and X_2 is the NDVI values.

Table 2. Performance of machine learning models.

Model	R-Squared (%)	Mean Absolute Error (MAE)
Polynomial Regression (Degree 2)	11	2.036
SVM (with RBF kernel)	7	2.033
Gradient Boosting Machine	10	2.044
Ridge	9.6	2.058
Linear Regression	9.6	2.058
OLS	7.5	2.058
Lasso	0.7	2.133
K-Nearest Neighbors	−4.0	2.197
Random Forest	−9.0	2.232
Decision tree	−78	2.940

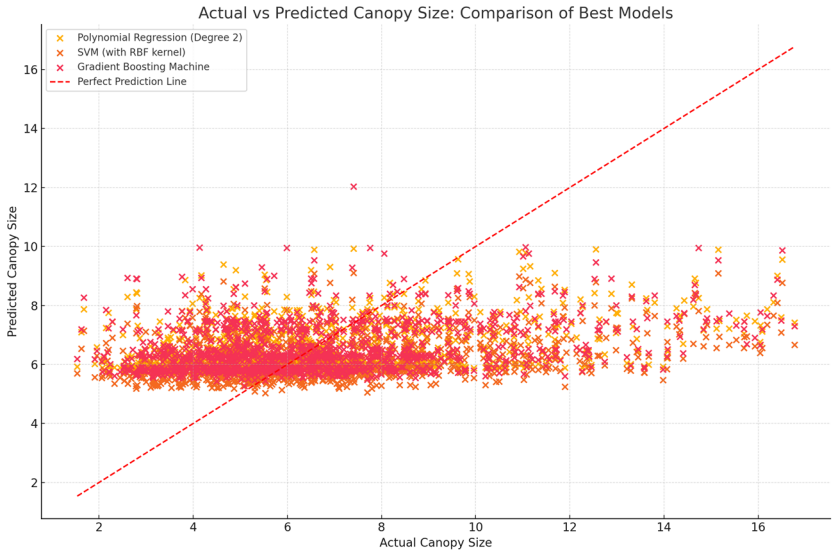

Figure 12. Predictive ability of SVM with RBF kernel, Polynomial Regression with Degree 2 models, and Gradient Boosting Machine. The red line represents perfect predictions. The closer the points are to this line, the more accurate the model's predictions.

4. Discussion

Our investigation into individual crop identification and canopy delineation, leveraging computational geometry via high-resolution UAV imagery, demonstrated exceptional effectiveness for precise crop boundary delineation and canopy structure characterization. By utilizing two distinct flight altitudes for data collection, we captured high-resolution, continuous RGB imagery that was critical for generating accurate 3D orthoimages essential for individual crop detection. While the RGB sensors delivered quality data, the integration of a hyperspectral sensor, as recommended by [29], could provide a richer geometrical representation, vital for enhancing crop detection capabilities.

The process of filtering the Canopy Height Model (CHM) was pivotal in eliminating noise during preprocessing, significantly bolstering the accuracy of our canopy size delineation. This aligns with improvements highlighted by [25,26], showcasing the evolution of methodologies in remote sensing. The careful selection of a plant height threshold was crucial, necessitating precision to ensure that vital features were not omitted while

achieving optimal results. Our geospatial analytical approach was successful in pinpointing individual crop peak heights, drawing parallels to CNNs' feature extraction capabilities in plant detection and classification as utilized by [23]. However, despite the strengths of CNNs, they encountered challenges in achieving precise crop delineation, underscoring the ongoing need to integrate domain-specific knowledge for enhanced accuracy. Our methodology facilitated necessary adjustments to address any data misrepresentations effectively. Employing the maximum functionality of our analytical tools enabled the discernment of individual crop tops through a detailed pixel-to-pixel comparison. Determining an optimal kernel size for the moving window, informed by domain knowledge regarding crop row spacing, was crucial in refining our analysis. The derived local peak heights were instrumental in creating Voronoi polygons for canopy delineation. This technique accurately demarcated crop boundaries and highlighted advancements in remote sensing and precision agriculture. Moreover, the resultant Voronoi diagrams not only facilitated a visual understanding of crop spatial organization but also enhanced the efficiency of subsequent agricultural interventions. This study has significantly enhanced crop monitoring and management practices and underscores the potential of the Voronoi diagram method in characterizing crop canopy structures. The effectiveness of this method, while proven in the context of this study, suggests a potential for broader applications, necessitating further research to evaluate its efficacy across diverse regions and cropping systems. Such research could explore the scalability of the Voronoi approach in larger, more heterogeneous landscapes and its integration with other technological advancements in precision agriculture. This could include the fusion of hyperspectral imaging and machine learning algorithms to create a more dynamic, responsive approach to crop management that adjusts to the varying conditions of different agricultural environments.

5. Conclusions

Our findings support the superiority of UAVs in acquiring plant information due to their high accuracy and their ability to overcome the limitations associated with traditional methods. UAVs provide high-resolution imagery that captures the field at various angles and times, offering a more comprehensive understanding of crop health and development. By leveraging the flexibility of UAV imagery, we were able to create accurate CHMs that provided a clear distinction between crop vegetation and soil, which facilitated automated discrimination between the two. The flexibility and effectiveness of the proposed method are evident in its ability to generate precise Canopy Height Models (CHMs), discriminate between vegetation and soil automatically, and select optimal moving window sizes based on the specific layout and structure of each field. The mean shift segmentation technique used for vegetation–soil discrimination significantly enhances this approach by reducing noise and refining the analysis, representing a substantial advancement in remote sensing-based crop analysis. Furthermore, the integration of computational geometry for canopy delineation, coupled with UAV imagery and advanced data processing, ensures a comprehensive assessment of the crop canopy structure. The accurate characterization of individual crop heights and boundaries offers a valuable tool for agronomists and farmers, enabling better resource management and tailored interventions that can ultimately improve crop yields. The use of the Voronoi diagram method illustrates how computational geometry can effectively enhance precision agriculture by providing high-resolution spatial analysis of crop structures. By combining this with advanced data processing techniques, such as mean shift segmentation and CHM filtering, this methodology is poised to deliver even more precise agricultural insights as it continues to evolve and adapt. Further research is necessary to assess its adaptability in varying geographical regions and cropping systems, potentially incorporating machine learning algorithms and hyperspectral imaging for even greater precision in crop detection and management.

Author Contributions: F.D. contributed to the conceptualization, data curation, formal analysis, methodology, visualization, original draft writing, software development, and investigation aspects of the study. L.H.-B. was involved in conceptualization, methodology development, acquiring funding,

project administration, resource management, supervision, validation, and the review and editing of the manuscript. All authors have read and agreed to the published version of the manuscript.

Funding: This work received partial support from the National Science Foundation under the grants "Developing a Robust, Distributed, and Automated Sensing and Control System for Smart Agriculture" [grant number 1832110], NOAA award NA21OAR4590358, and NASA award 80NSSC23M0051, and NSF grant 1800768.

Data Availability Statement: The data supporting this study's findings are available from the authors upon reasonable request.

Acknowledgments: We extend our gratitude to the team responsible for piloting the UAVs during the data collection phase of our study.

Conflicts of Interest: The authors declare no competing financial interests or personal relationships that could have influenced the work reported in this paper.

References

1. McConnell, M.D. Bridging the gap between conservation delivery and economics with precision agriculture. *Wildl. Soc. Bull.* **2019**, *43*, 391–397. [CrossRef]
2. Higgins, V.; Bryant, M.; Howell, A.; Battersby, J. Ordering adoption: Materiality, knowledge and farmer engagement with precision agriculture technologies. *J. Rural Stud.* **2017**, *55*, 193–202. [CrossRef]
3. Cisternas, I.; Velásquez, I.; Caro, A.; Rodríguez, A. Systematic literature review of implementations of precision agriculture. *Comput. Electron. Agric.* **2020**, *176*, 105626. [CrossRef]
4. Beland, M.; Parker, G.; Sparrow, B.; Harding, D.; Chasmer, L.; Phinn, S.; Antonarakis, A.; Strahler, A. On promoting the use of lidar systems in forest ecosystem research. *For. Ecol. Manag.* **2019**, *450*, 117484. [CrossRef]
5. Elikem, D.F.; Leila, H.-B.; Ali, K.; Abolghasem, S. UAV Remote Sensing Assessment of Crop Growth. *Photogramm. Eng. Remote Sens.* **2021**, *87*, 891–899.
6. Sun, Q.; Sun, L.; Shu, M.; Gu, X.; Yang, G.; Zhou, L. Monitoring maize lodging grades via unmanned aerial vehicle multispectral image. *Plant Phenomics* **2019**, *2019*, 5704154. [CrossRef] [PubMed]
7. Yurtseven, H.; Akgul, M.; Coban, S.; Gulci, S. Determination and accuracy analysis of individual tree crown parameters using UAV based imagery and OBIA techniques. *Measurement* **2019**, *145*, 651–664. [CrossRef]
8. Wan Mohd Jaafar, W.S.; Woodhouse, I.H.; Silva, C.A.; Omar, H.; Abdul Maulud, K.N.; Hudak, A.T.; Klauberg, C.; Cardil, A.; Mohan, M. Improving individual tree crown delineation and attributes estimation of tropical forests using airborne LiDAR data. *Forests* **2018**, *9*, 759. [CrossRef]
9. Mohan, M.; Mendonça, B.; Silva, C.; Klauberg, C.; de Saboya Ribeiro, A.S.; Araújo, E.; Monte, M.A.; Cardil, A. Optimizing individual tree detection accuracy and measuring forest uniformity in coconut (*Cocos nucifera* L.) plantations using airborne laser scanning. *Ecol. Model.* **2019**, *409*, 108736.
10. Dorbu, F.E.; Beni, L.H. Geospatial Intelligence for Individual Crop Detection and Anomaly Monitoring. In Proceedings of the IGARSS 2023—2023 IEEE International Geoscience and Remote Sensing Symposium, Pasadena, CA, USA, 16–21 July 2023; pp. 1051–1054.
11. Wilke, N.; Siegmann, B.; Klingbeil, L.; Burkart, A.; Kraska, T.; Muller, O.; van Doorn, A.; Heinemann, S.; Rascher, U. Quantifying lodging percentage and lodging severity using a UAV-based canopy height model combined with an objective threshold approach. *Remote Sens.* **2019**, *11*, 515. [CrossRef]
12. Wang, Z.; Nie, C.; Wang, H.; Ao, Y.; Jin, X.; Yu, X.; Bai, Y.; Liu, Y.; Shao, M.; Cheng, M.; et al. Detection and analysis of degree of maize lodging using UAV-RGB image multi-feature factors and various classification methods. *ISPRS Int. J. Geo-Inf.* **2021**, *10*, 309. [CrossRef]
13. Malachy, N.; Zadak, I.; Rozenstein, O. Comparing methods to extract crop height and estimate crop coefficient from UAV imagery using structure from motion. *Remote Sens.* **2022**, *14*, 810. [CrossRef]
14. Liu, X.; Bo, Y. Object-based crop species classification based on the combination of airborne hyperspectral images and LiDAR data. *Remote Sens.* **2015**, *7*, 922–950. [CrossRef]
15. Dobosz, B.; Gozdowski, D.; Koronczok, J.; Žukovskis, J.; Wójcik-Gront, E. Evaluation of Maize Crop Damage Using UAV-Based RGB and Multispectral Imagery. *Agriculture* **2023**, *13*, 1627. [CrossRef]
16. Aeberli, A.; Johansen, K.; Robson, A.; Lamb, D.W.; Phinn, S. Detection of banana plants using multi-temporal multispectral UAV imagery. *Remote Sens.* **2021**, *13*, 2123. [CrossRef]
17. Jing, L.; Hu, B.; Noland, T.; Li, J. An individual tree crown delineation method based on multi-scale segmentation of imagery. *ISPRS J. Photogramm. Remote Sens.* **2012**, *70*, 88–98. [CrossRef]
18. Marasigan, R.; Festijo, E.; Juanico, D.E. Mangrove crown diameter measurement from airborne lidar data using marker-controlled watershed algorithm: Exploring performance. In Proceedings of the 2019 IEEE 6th International Conference on Engineering Technologies and Applied Sciences (ICETAS), Kuala Lumpur, Malaysia, 20–21 December 2019.

19. Huang, H.; Li, X.; Chen, C. Individual tree crown detection and delineation from very-high-resolution UAV images based on bias field and marker-controlled watershed segmentation algorithms. *IEEE J. Sel. Top. Appl. Earth Obs. Remote Sens.* **2018**, *11*, 2253–2262. [CrossRef]
20. Jensen, J.L.; Mathews, A.J. Assessment of image-based point cloud products to generate a bare earth surface and estimate canopy heights in a woodland ecosystem. *Remote Sens.* **2016**, *8*, 50. [CrossRef]
21. Gao, M.; Yang, F.; Wei, H.; Liu, X. Individual maize location and height estimation in field from UAV-Borne lidar and rgb images. *Remote Sens.* **2022**, *14*, 2292. [CrossRef]
22. Varela, S.; Dhodda, P.R.; Hsu, W.H.; Prasad, P.V.V.; Assefa, Y.; Peralta, N.R.; Griffin, T.; Sharda, A.; Ferguson, A.; Ciampitti, I.A. Early-season stand count determination in corn via integration of imagery from unmanned aerial systems (UAS) and supervised learning techniques. *Remote Sens.* **2018**, *10*, 343. [CrossRef]
23. Fujimoto, A.; Haga, C.; Matsui, T.; Machimura, T.; Hayashi, K.; Sugita, S.; Takagi, H. An end to end process development for UAV-SfM based forest monitoring: Individual tree detection, species classification and carbon dynamics simulation. *Forests* **2019**, *10*, 680. [CrossRef]
24. Miraki, M.; Sohrabi, H.; Fatehi, P. Detection of mistletoe infected trees using UAV high spatial resolution images. *J. Plant Dis. Prot.* **2021**, *128*, 1679–1689. [CrossRef]
25. Abd-Elrahman, A.; Guan, Z.; Dalid, C.; Whitaker, V.; Britt, K.; Wilkinson, B.; Gonzalez, A. Automated canopy delineation and size metrics extraction for strawberry dry weight modeling using raster analysis of high-resolution imagery. *Remote Sens.* **2020**, *12*, 3632. [CrossRef]
26. Valluvan, A.B.; Raj, R.; Pingale, R.; Jagarlapudi, A. Canopy height estimation using drone-based RGB images. *Smart Agric. Technol.* **2023**, *4*, 100145. [CrossRef]
27. Alface, A.B.; Pereira, S.B.; Filgueiras, R.; Cunha, F.F. Sugarcane spatial-temporal monitoring and crop coefficient estimation through NDVI. *Rev. Bras. Eng. Agrícola E Ambient.* **2019**, *23*, 330–335. [CrossRef]
28. Hashemi-Beni, L.; Kurkalova, L.A.; Mulrooney, T.J.; Azubike, C.S. Combining Multiple Geospatial Data for Estimating Above-ground Biomass in North Carolina Forests. *Remote Sens.* **2021**, *13*, 2731. [CrossRef]
29. Hashemi-Beni, L.; Gebrehiwot, A.; Karimoddini, A.; Shahbazi, A.; Dorbu, F. Deep convolutional neural networks for weeds and crops discrimination from UAS imagery. *Front. Remote Sens.* **2022**, *3*, 755939. [CrossRef]
30. Aeberli, A.; Phinn, S.; Johansen, K.; Robson, A.; Lamb, D.W. Characterisation of Banana Plant Growth Using High-Spatiotemporal-Resolution Multispectral UAV Imagery. *Remote Sens.* **2023**, *15*, 679. [CrossRef]
31. Mostafavi, M.A.; Beni, L.H.; Mallet, K.H. Geosimulation of geographic dynamics based on voronoi diagram. In *Transactions on Computational Science IX*; Springer: Berlin/Heidelberg, Germany, 2010.
32. Beni, L.H. Development of a 3D Kinetic Data Structure Adapted for a 3D Spatial Dynamic Field Simulation. Ph.D. Thesis, Laval University, Quebec City, QC, Canada, 2009.
33. Hashim, H.; Latif, Z.A.; Adnan, N.A. Urban vegetation classification with NDVI threshold value method with very high resolution (VHR) Pleiades imagery. *Int. Arch. Photogramm. Remote Sens. Spat. Inf. Sci.* **2019**, *42*, 237–240. [CrossRef]
34. St. Peter, J.; Hogland, J.; Hebblewhite, M.; Hurley, M.A.; Hupp, N.; Proffitt, K. Linking phenological indices from digital cameras in idaho and montana to MODIS NDVI. *Remote Sens.* **2018**, *10*, 1612. [CrossRef]
35. Reid, A.M.; Chapman, W.K.; Kranabetter, J.M.; Prescott, C.E. Response of lodgepole pine health to soil disturbance treatments in British Columbia, Canada. *Can. J. For. Res.* **2015**, *45*, 1045–1055. [CrossRef]
36. Yang, J.; Xing, M.; Tan, Q.; Shang, J.; Song, Y.; Ni, X.; Wang, J.; Xu, M. Estimating effective leaf area index of winter wheat based on uav point cloud data. *Drones* **2023**, *7*, 299. [CrossRef]
37. Chauhan, S.; Darvishzadeh, R.; Boschetti, M.; Nelson, A. Estimation of crop angle of inclination for lodged wheat using multi-sensor SAR data. *Remote Sens. Environ.* **2020**, *236*, 111488. [CrossRef]
38. Chauhan, S.; Darvishzadeh, R.; Boschetti, M.; Pepe, M.; Nelson, A. Remote sensing-based crop lodging assessment: Current status and perspectives. *ISPRS J. Photogramm. Remote Sens.* **2019**, *151*, 124–140. [CrossRef]